

Towards *Physarum* Engines

Soichiro Tsuda, Jeff Jones, and Andrew Adamatzky

Unconventional Computing Centre,
University of the West of England,
Bristol BS16 1QY, United Kingdom

Published in:

Tsuda S., Jones J., Adamatzky A.
Towards *Physarum* engines.
Applied Bionics and Biomechanics 9 (2012) 3, 221-240.

Abstract

The slime mould *Physarum polycephalum* is a suitable candidate organism for soft-matter robotics because it exhibits controllable transport, movement and guidance behaviour. *Physarum* may be considered as a smart computing and actuating material since both its motor and control systems are distributed within its undifferentiated tissue and can survive trauma such as excision, fission and fusion of plasmodia. Thus it may be suitable for exploring the generation and distribution of micro-actuation in individual units or planar arrays. We experimentally show how the plasmodium of *Physarum* is shaped to execute controllable oscillatory transport behaviour applicable in small hybrid engines. We measure the lifting force of the plasmodium and demonstrate how protoplasmic transport can be influenced by externally applied illumination stimuli. We provide an exemplar vehicle mechanism by coupling the oscillations of the plasmodium to drive the wheels of a Braitenberg vehicle and use light stimuli to effect a steering mechanism. Using a particle model of *Physarum* we show how emergent travelling wave patterns produced by competing oscillatory domains may be used to generate spatially represented actuation patterns. We demonstrate different patterns of controllable motion, including linear, reciprocal, rotational and helical, and demonstrate in simulation how dynamic oscillatory patterns may be translated into motive forces for simple transport of substances within a patterned environment.

Keywords: true slime mould, biological robotics, soft matter, non-silicon motors

*Unconventional Computing Centre, University of the West of England, Bristol BS16 1QY, United Kingdom

1 Introduction

Very small scale mechanisms made possible by recent advances in micro-fabrication still require a means of energy conversion to convert a fuel supply into useful motive force. Although it is possible to reduce conventional engines and transmission designs in scale, doing so introduces challenges with regard to friction [16], heat [9] and more general miniaturisation problems [33] that may differ from or exacerbate those observed at the larger scale. Recent approaches have sought inspiration from biological sources of to provide the transformation of energy conversion to motive force, examples from flagellated movement of bacteria [48] and eukaryotes [15], ciliated transport for microscopic mixing [13] and transport [35], peristaltic propulsion [39, 32], amoeboid movement [43] and collective mass transport [25] have all been suggested.

Biologically inspired mechanisms are attractive since they are composed of simple and plentiful materials and show impressive feats of redundancy, fault tolerance and self repair. However, even though the above mechanisms are technologically elegant and the product of impressive biological self-assembly, the internal arrangement of components underlying some mechanisms — for example the bacterial flagellar motor system — are as complex as those in non-biological machines. Progress in the development of biologically inspired machines has also been made by considering the use of even more simple biological structures which straddle the boundary of non-living physical materials and living organisms. Such structures include biological fibres and membranes [49], lipid self assembly in terms of networks [27], pseudopodium-like membrane extension [28] and even basic chemotaxis response [26].

Of particular interest are materials which embody oscillatory states, since the periodic transitions between two or more states can provide differential behaviour and impetus, if suitably coupled to a propulsion mechanism. The resulting transport may be relatively simple, such as flagellar or ciliary motion [14], or as complex as the patterns produced by neural assemblies of central pattern generators [20]. When oscillatory states are combined with local communication waves of excitation may propagate which can also result in motion if the excitation is coupled to propulsion mechanism. Reaction-diffusion phenomena have proven to be useful in this approach because the emergence of oscillatory states can be a self organised and robust process and also feature travelling wave phenomena. Reaction-diffusion approaches to robotics include the use of propagating waves for robotic control and navigation [5], for the manipulation and transport of objects [6], and oscillatory wave transport within a gel-like material for forward movement [29].

Biological (complete living systems) and semi-biological (materials produced by living systems) approaches can each provide valuable insights and techniques in the pursuit of small scale machines. The ideal hypothetical candidate for a biological machine would be an organism which is capable of the complex sensory integration, movement and adaptation of a living organism, yet which is also composed of a relatively simple material that is amenable to simple understanding and control of its properties.

We suggest that the myxomycete organism, the true slime mould *Physarum polycephalum*, is a suitable candidate organism which meets both criteria; i.e. it is a complex organism, but which is composed of relatively simple materials. A giant single-celled organism, *Physarum* is an attractive biological candidate medium for emergent motive force because the basic physical mechanism during the plasmodium stage of its life cycle is a self-organised system of oscillatory contractile activity which is used in the pumping and distribution of nutrients within its internal transport network. The organism is remarkable in that the control of the oscillatory behaviour is distributed throughout the almost homogeneous medium and is highly redundant, having no critical or unique components.

The plasmodium of *Physarum* is amorphous, jelly-like and flat in appearance and ranges from the microscopic scale to up to many square metres in size. The plasmodium is a single cell formed by repeated nuclear division and is comprised of a sponge-like actin-myosin mesh-work presented in two physical phases. The gel phase is a dense matrix subject to spontaneous contraction and relaxation under the influence of changing concentrations of intracellular chemicals. The sol phase is a liquid protoplasm transported through the plasmodium by the force generated by the oscillatory contractions within the gel matrix. There is a complex interplay between the gel and sol phases and both phases can change between each form when subject to changes in pressure, temperature, humidity and local transport. The internal structure of *Physarum* can thus be regarded as a complex functional material capable of both sensory and motor behaviour. Indeed *Physarum* has been described as a membrane bound reaction-diffusion system [1] in reference to both the complex interactions within the plasmodium and the rich computational properties afforded by its 'material' properties [7, 4].

From a robotics perspective it has previously been shown that plasmodium of *Physarum*, by its adaptation to changing conditions within its environment, may be considered as a prototype micro-mechanical manipulation system, capable of simple and programmable robotic actions including the manipulation (pushing and pulling) of small scale objects [8, 4], light-controlled propelling of small floating objects [2, 4], peristaltic transporter (intelligent self-growing pipe) of biologically friendly substances [4, 3], and as a guidance mechanism in a biological/mechanical hybrid approach where the response of the plasmodium to light irradiation was used to provide feedback control to a robotic system [42]. A *Physarum* inspired approach to robotics using amoeboid movement generated by a series of fluid coupled oscillators has been also been demonstrated [43].

In this report we discuss the use of *Physarum* as a candidate organism and material for the spontaneous generation and distribution of physical forces for engine-like and distributed planar transport mechanisms. The layout of the paper is as follows. Section 2 shows experimental results demonstrating that *Physarum* plasmodium is capable of generating motive lifting force which is both measurable and externally controllable. Using a dumbbell patterned design we demonstrate complex phase relationships from the oscillatory dynamics and we design a prototype example mechanism where the motive output of *Physarum* plasmodium oscillations is used to drive the wheels of a simulated

Braitenberg vehicle, using external light stimuli to steer the vehicle. Building upon the experimental results we investigate in Sect. 3 the emergence of oscillatory transport in the computational modelling of a virtual material composed of a particle collective where — as with the plasmodium — oscillatory phenomena emerge from simple and local interactions. Building on the so-called ‘smart table’ approach in [6], we suggest a *Physarum* inspired method of generating wave based transport by patterning a planar environment into predefined shapes. In Sect. 4 we demonstrate a range of transport types (linear, rotary, reciprocal and helical) and coupling methods using this approach. We also demonstrate in simulation how the emergent oscillatory patterns in the model may be interpreted as a vector field to transport material within patterned regions. We summarise the experimental and theoretical findings in Sect. 5 and suggest future research by which small scale transport devices may be constructed from materials which exhibit emergent properties from simple component interactions.

2 Experimental

This section focus on experimental investigation into the possibility of *Physarum* engine implementation. The *Physarum* plasmodium is famously known for fast protoplasmic streaming within the cell body and the motive force of the cell has been studied extensively in the field of cell biology for more than 50 years (cf. [10, 23, 18]). The mechanism of streaming generation is based on the actin polymerization/depolymerization cycle, which switches every 30 s regulated by calcium ions [34]. This periodic cycle controls the direction of the protoplasmic streaming, and as a result, the whole cell shows rhythmic cell thickness changes [23]. The flow speed of protoplasmic streaming of the plasmodium becomes up to 1 mm/s, whereas that of other organisms, such as plant and amoeba cells, are about tens of $\mu\text{m/s}$ [24]. This is one of the fastest protoplasmic streaming known so far, and together with the periodicity of the protoplasmic streaming, the plasmodium of *Physarum* could be ideal candidate to fabricate small-scale biological devices, e.g. actuator and transporter.

In order to explore the possibility of using the *Physarum* cell as source of power, it is important to know (a) how much force a *Physarum* plasmodium can generate, and (b) how the force can be steered externally. Before going to these two points, we first discuss characteristics of the cell shape and the contraction oscillation rhythm in the *Physarum* plasmodium.

2.1 Cell Shape and Oscillation Pattern

The generation of periodic rhythm of the cell confined in a small circular well on the agar gel was investigated by the authors and also other researchers previously [41, 36]. When observed under a microscope, a piece of *Physarum* cell just placed in the well consists of smaller pieces of granular protoplasm, each of which can potentially become an individual slime mold cell. These granules start contracting about 10 min after transplanted and neighboring granules

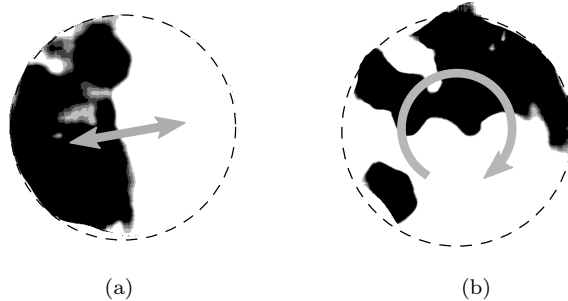


Figure 1: Oscillation patterns of the *Physarum* plasmodium in a single well: (a) bilateral shuttle oscillation and (b) clockwise rotation wave. Black and white regions indicate areas where thickness is increasing and decreasing, respectively.

gradually merge together to synchronize the contraction rhythm. They eventually fuse into one single *Physarum* plasmodium and show several types of synchronized oscillation rhythms, such as bilateral shuttle streaming of protoplasm (Fig. 1a) and clockwise or anti-clockwise rotation streaming (Fig. 1b). What is remarkable about the oscillation regeneration in the *Physarum* plasmodium is “size-invariant” behavior. Even if the cell size becomes larger with increased size of well, a whole cell fully synchronizes relatively quickly. We undertook experiments with 1.5, 3.0, 4.5, 6.0, and 7.5 mm diameter wells, and in all cases the *Physarum* cell fully synchronized approximately in 70 min [41]. Thus the plasmodium is good at coordinating the internal structure while maintaining itself as a single cell. Even when the body size changes, the plasmodium restores the synchronization using a distributed-computing type control.

Although a cell in the well does show oscillations that potentially can be exploited as source of power, the single well design would not be appropriate for *Physarum* engine. Given that a whole plasmodium in a well is used to apply force to another object, a total displacement (i.e. thickness change) of the cell will be crucial. However, in the case of single well, the total displacement will be balanced out. For example, if a cell is showing bilateral oscillation (Fig. 1a), the thickness of a half of the cell is increasing while that of the other half is decreasing. As a result, the total displacement becomes almost zero. This fact led us to the design of a dumb-bell shape, in which two circular wells are connected by a narrow channel, see Fig. 4a. This design is originally made by Takamatsu et al [37]. When the width of the connecting channel is 0.4 mm, anti-phase thickness oscillation between two wells can be observed [38]. This means protoplasm of the cell flows back and forth between wells, and thus the thickness displacement in one well will not be canceled out.

Therefore we adopt the dumb-bell shape design and keep the cell to take the shape by hydrophobic structures. A plasmodium prefers high-humidity niche and it stays inside the structures of wet-wells and keeps its shape for a long time. *Physarum* cells used for experiments below were cultured on 1.5 % agar

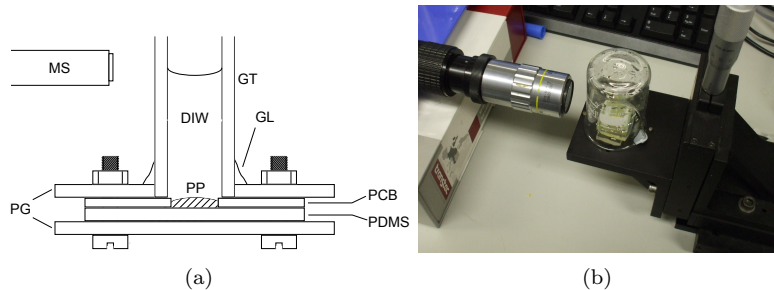


Figure 2: Experimental setup for plasmodium force measurement: (a) A schematic illustration of plasmoidal force measurement setup. MS: Microscope, GT: Glass tube, DIW: Distilled water, GL: Glue, PP: *Physarum* plasmodium, PG: Plexi glass, PCB: Printed circuit board, PDMS: Polydimethylsiloxane silicon rubber. (b) A photo of the setup.

gel in the thermostatic chamber (Lucky Reptile Herp Nursery II Incubator, Net Pet Shop, UK) at 26°C and fed with oat flakes once or twice a day. They were starved at least for 12 hours prior to experiments.

2.2 Force generated by plasmodium

Let us evaluate how much force could be generated plasmodium’s oscillatory contractions. We estimate the force by loading some weight on a plasmodium: we load water one of two wells of a dumb-bell shaped plasmodium (Fig. 2a). By changing the height of water, the load on the cell is controlled.

A dumb-bell shaped plasmodium was prepared as follows. Small pieces of *Physarum* are taken from a larger culture and set in dumb-bell shaped wells of a thin printed circuit board (PCB), with copper coating removed. They are then placed on a 1.5 % agar gel and kept in a dark place at least for two hours so that the pieces of *Physarum* fuse into one single cell. After the fusion occurs, the cell and the PCB are clamped together with plexiglass and a PDMS block (Fig. 2a). A glass tube, which inner diameter is same as the diameter of a plasmodium well, is glued to the top plexi glass and filled with distilled water to a certain height. The whole setup is covered with a wet glass beaker to avoid evaporation of water in the glass tube and placed on the three-dimensional micro-stage (Fig. 2b). The displacement of water surface is recoded for 20 min by a microscope from the size.

Figure 3a shows a result of surface displacement experiment in the case of 100 mm water height. We have tested with 40, 60, 80, and 100 mm water height (71, 106, 141, and 177 mg in weight, respectively).

In all the cases the height of water surface periodically oscillates due to the thickness oscillation of the plasmodium at the bottom. When no load is placed on the slime mould, it showed thickness oscillations of approximately 60s per cycle, which is a typical oscillation period of the *Physarum* plasmodium.

When DIW weight was added on the cell, on the other hand, the period became longer up to twofold. The more load the slime mould carries, the slower the period became. For example, a typical period was 65s and 90s per cycle for 20mm and 60mm-high water weight, respectively. Even at the maximum load, 100mm-high case, it was around 100s per cycle, as shown in Fig.3a. During an experiment with a fixed load, the period slowed down gradually and slightly. In many cases, water height slightly decreased (approximately 10–40 μm) during a 20 min experiment. This is possibly because the *Physarum* cell partially escaped to the side of the well not connected to the water tube. The maximum displacement of water surface was estimated by detecting peaks and bottoms of the oscillation (marked as “*” in Figure 3a) and calculated differences from a bottom to the next peak. Figure 3b summarizes the maximum displacement of various water heights. As the water height becomes higher, the displacement decreases monotonically. By extrapolating this result, the maximum height the dumb-bell shaped plasmodium could bear with would be 140 mm, and it could lift up to approximately 250mg load.

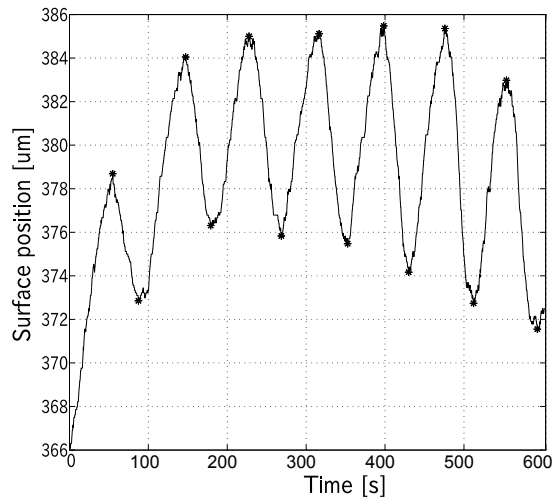
The work by the plasmodium in the case of 100 mm water height can be calculated as $W = (0.75)^2 \times \pi \times 100 \times \rho \times g \times 0.007 \approx 12.1$ (mJ), where ρ is the density of water (1mg/mm³) and g is the gravity acceleration (9.8 m/s²). Assuming that the speed of thickness change is constant, the power of the cell can be estimated as $P = W/T = 12.1/50 \approx 0.24$ (mW).

At the micron scale, however, one has to bear in mind that some factors, which do not need to be considered at a macro scale, become crucial. For example, friction becomes relatively large compared to the force generated by the cell. Thus, for the effective use of the force, a careful attention to things like a choice of lubricant and the design of stop valve have to be paid. Nevertheless, it is noteworthy that a tiny cell, which weight approximately 5 mg, can lift up a load over 36 times heavier than its own weight. Such strong force generated by the *Physarum* plasmodium was in fact reported more than three decades ago by several researchers [47, 45].

2.3 Steering Control of *Physarum* Engine

There are several ways to externally stimulate the *Physarum* ’s oscillation, such as light [19], temperature [46], and electric stimuli [11]. Among others, light stimulus is the most commonly used one because it can be easily introduced or removed simply by switching light on and off. It is known that, when a local part of a plasmodium is exposed to white light, the frequency of thickness oscillation at the local part decreases [31]. Hence we adopt white light as external controller for steering of *Physarum* engine.

To confirm if white light affects the oscillation rhythm of the dumb-bell shaped cell, we conducted the following experiment. The dumb-bell shaped plasmodium is constructed on on a 1.5 % agar gel using a transparency sheet mask (Fig. 4a). The dumb-bell shaped hole in the mask was cut out with a 1/16” hand punch, which makes approximately 1.5 mm diameter hole, and the connecting channel in was cut with a scalpel under a stereo-microscope. The



(a)

Water height	Max. displacement
40 mm	20 μm
60 mm	14 μm
80 mm	10 μm
100 mm	7 μm

(b)

Figure 3: (a) A time course of the surface displacement in the case of 100 mm water height. First 10 min is shown. (b) A table of the maximum water displacement with different water height. It decreases monotonically as the water height increases.

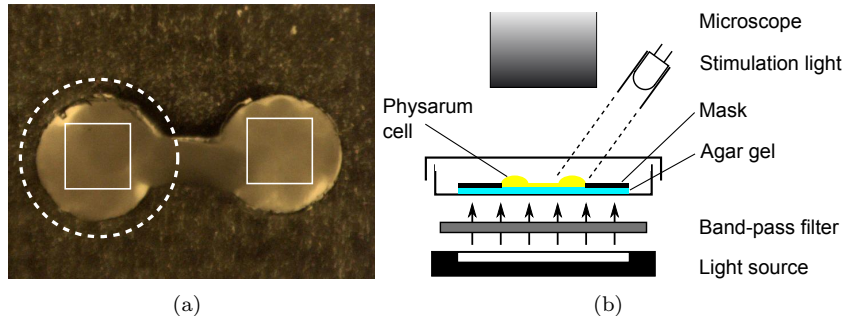


Figure 4: (a) A dumb-bell shaped plasmodium on a 1.5% agar gel. The black mask surrounding the cell is made of transparency sheet. A dotted circle indicates the area exposed to white light. The areas indicated by two solid squares are used to calculate thickness oscillations of the cell. (b) A schematic illustration of light illumination experiment. The cell is exposed to bandpass-filtered light from the bottom for monitoring and one of two wells is exposed to white LED light from the top for stimulation. The cell is kept in a Petri dish to maintain constant humidity condition.

structure is placed under a microscope (Leica Zoom 2000, Germany) and illuminated from the bottom with bandpass-filtered light near the 600 nm wavelength (Fig. 4b). This wavelength of light does not affect the *Physarum*'s oscillation activity [30]. The thickness of the cell is measured by the light transmission through the cell, which is inversely proportional to the thickness. The controller, an ultra bright white LED, illuminates only one of two wells of the plasmodium (a dotted circle in Fig. 4a). A snapshot image of the cell is saved every 3 s in a PC for subsequent image analysis.

The thickness of the cell is calculated as follows. We convert snapshots from RGB to gray scale, and then calculate a difference of images taken at t and $t - \Delta t_1$. This gives us a thickness change of the plasmodium in Δt (we used $\Delta t_1 = 7$). Then we apply a moving average filter spatially over 91×91 pixels (indicated by a solid square in Fig. 4a) and temporally over 15 images on each well. This works as an image smoothing filter to reduce camera noise.

Figure 5 shows a typical reaction of the cell to white light. Before the light is switched on the oscillations in two wells are synchronized in amplitude and phase (the first half of Fig. 5). When one of the wells becomes exposed to the light, the oscillations in wells go out of phase.

Light is a negative stimulus to *Physarum* and slows down the contractile oscillation at the illuminated part of a plasmodium. Period of oscillations becomes longer in the latter half of the plot in Fig. 5, whereas those of unexposed well remain unchanged.

Another reaction of the cell to the light is significant change in oscillation amplitudes. That in the stimulated well decreased largely soon after the light

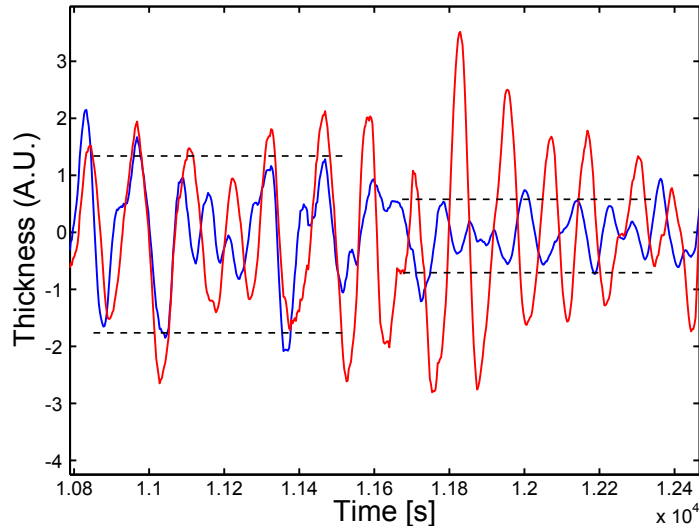


Figure 5: A typical reaction of the *Physarum* plasmodium to light stimulus. Only one of two wells is exposed to white light (blue curve). A LED light is turned on at the point indicated by a downward arrow and kept on till the end of the plot. The oscillation period of the stimulated well (blue curve) becomes slightly longer when the light is on, whereas that of the unstimulated well (red curve) remains unchanged. The oscillation amplitude significantly decreases in the stimulated well and increases in the other well (horizontal lines).

is turned on (indicated by horizontal dotted lines in Fig. 5), but on the other hand, that in the non-stimulated well increased. This is because the cell is trying to escape from the exposed area by actively pumping the protoplasm from the stimulated well to non-stimulated well. When white light is removed, the oscillation at the stimulated well came back to the original period and oscillation amplitudes in both wells equalize. Thus, white light does slow down the dumb-bell shaped *Physarum* plasmodium, and with this light stimulus, the cell can be steered from the outside. We are going to show a stimulated vehicle driven by the *Physarum* cell can be actually steered by light in the next section.

2.4 Vehicle simulation driven by experimental data

We assume that the power generated by a *Physarum* plasmodium is converted to drive wheels of a hypothetical micro-scale vehicle without any energy loss. Increases and decreases in thickness oscillations from two wells (Fig. 4a) drive wheels of a Braitenberg-like vehicles [12] illustrated in Fig. 6a. The vehicle has two wheels driven by oscillations of a dumb-bell-shaped plasmodium. It also has two lights which illuminate two wells of the cell integrated in the vehicle in

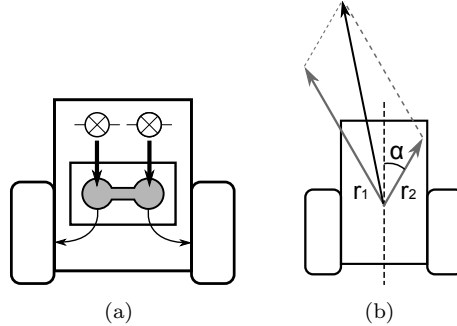


Figure 6: (a) A schematic diagram of a vehicle driven by *Physarum* engine. The oscillation amplitudes of the cell determines the wheel rotation speed of the vehicle. Light illumination onto each well of a *Physarum* plasmodium is used to steer the vehicle. (b) The motion of *Physarum*-driven simulated vehicle. Vehicle's direction of movement can be represented as addition of vectors (Eq. 1).

order to steer the vehicle.

There are several outputs of the thickness oscillation that can be used to drive the wheels. For example, thickness amplitude, oscillation frequency, and phase difference between oscillations of two wells. Here we employ thickness amplitude to demonstrate vehicle control. We assume that the thickness oscillation pushes a hypothetical piston and rotates a crankshaft to change the speed of one of wheels. The wheels rotate at a constant speed and the thickness oscillations of the cell increases the speed depending on the amplitude. The motion of a *Physarum*-driven vehicle is illustrated in Fig. 6b):

$$\begin{cases} x(t+1) &= x(t) + |r_1|\sin(\theta + \alpha) + |r_2|\sin(\theta - \alpha) \\ y(t+1) &= y(t) + |r_1|\cos(\theta + \alpha) + |r_2|\cos(\theta - \alpha) \end{cases} \quad (1)$$

where $x(t)$ and $y(t)$ are positions of the vehicle at time t , and r_1, r_2 are thickness displacement of the cell in left and right wells in a certain period (in this case, 21 s). α is a parameter that determines the contribution of the thickness displacement to the change of wheel running speed. The larger α is, the more wheels are accelerated. Hence, with larger α , vehicle's direction of movement becomes more sensitive to the difference of oscillation amplitudes from two wells (i.e. if $\| |r_1| - |r_2| \|$ is large, the vehicle turns either to the left or right).

Figure 7 shows a trajectory of the simulated vehicle driven by experimental data. The vehicle started from the origin (0,0) goes straight (black line) when no light inputs are on. It turns to the left (red line) as soon as the left well of the dumb-bell-shaped cell is stimulated by light. When light is turned off, it drives straight ahead again. This can be explained as follows in terms of *Physarum*'s behavior. When there is no stimulus to the cell, both wells oscillates with same amplitude (cf. Fig. 5). This drives the wheels with the same speed, and thus the vehicle goes straight. On the other hand, as described in the

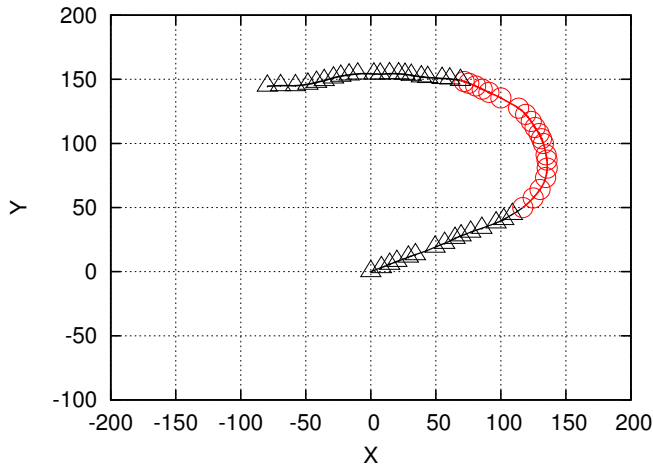


Figure 7: Trajectory of the simulated vehicle driven by experimental data. $\alpha = \pi/720$ is used in this simulation. The vehicle started from (0,0). Black line indicates the period when there is no light illumination to wells, and red line is when a right well is illuminated by light.

previous section, the oscillation amplitude in the stimulated well significantly decreases while the light is on, whereas that in the other well increases. This is because the cell moves out of the illuminated area and migrates towards the non-illuminated well. This slows down the left wheel driven by the stimulated well and accelerates the right wheel. As a result, the vehicle takes a left turn as long as the light is on. It drives in a straight line again after the light is turned off because oscillation amplitudes in two wells come back to nearly equal level when light stimulation is removed.

3 The Emergence of Oscillatory Transport Phenomena in a Particle-Based Model

Due to the relatively slow time development of the *Physarum* plasmodium and natural variability of its 'performance' in terms of the chosen robotics tasks (the plasmodium is only concerned with survival and not, after all, with satisfying externally applied experimental tasks), it is helpful to develop computational modelling approaches which may facilitate the study of distributed robotic control. Such a modelling approach allows us to explore the emergence of complex oscillatory behaviour from simple components and assess its application to robotics tasks.

To investigate the use of emergent oscillatory phenomena for engine-like transport we employ an extension to the particle model in [22] which was shown to generate dynamical emergent transport networks. In this approach

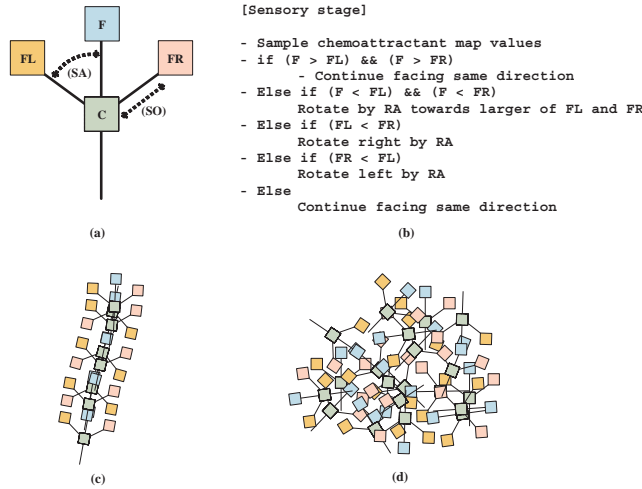


Figure 8: Agent particle morphology, algorithm, and aggregation types.

a plasmodium is composed of a population of mobile particles with very simple behaviours, residing within a 2D diffusive environment. A discrete 2D lattice (where the features of the environment arena are mapped to greyscale values in a 2D image) stores particle positions and also the concentration of a local factor which we refer to generically as chemoattractant. The 'chemoattractant' factor actually represents the hypothetical flux of sol within the plasmodium. Free particle movement represents the sol phase of the plasmodium. Particle positions represent the fixed gel structure (i.e. global pattern) of the plasmodium. Particles act independently and iteration of the particle population is performed randomly to avoid introducing any artifacts from sequential ordering. Particle behaviour is divided into two distinct stages, the sensory stage and the motor stage. In the sensory stage, the particles sample their local environment using three forward biased sensors whose angle from the forwards position (the sensor angle parameter, SA), and distance (sensor offset, SO) may be parametrically adjusted (Fig. 8a). The offset sensors represent the overlapping and inter-twining filaments within the transport networks and plasmodium, generating local coupling of sensory inputs and movement (Fig. 8c and d).

The SO distance is measured in pixels and a minimum distance of 3 pixels is required for strong local coupling to occur. During the sensory stage each particle changes its orientation to rotate (via the parameter rotation angle, RA) towards the strongest local source of chemoattractant (Fig. 8b). After the sensory stage, each particle executes the motor stage and attempts to move forwards in its current orientation (an angle from 0-360°) by a single pixel forwards. Each lattice site may only store a single particle and-critically-particles deposit chemoattractant into the lattice only in the event of a successful forwards movement (Fig. 9a). If the next chosen site is already occupied by another

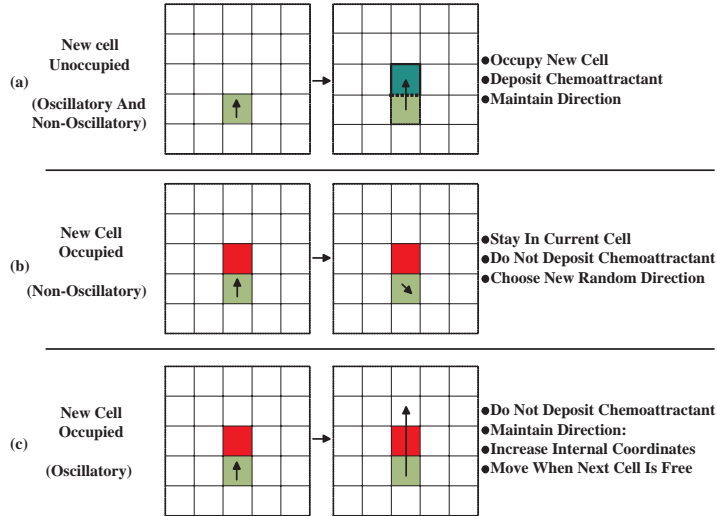


Figure 9: Particle motor behaviour in non-oscillatory and oscillatory conditions

particle the default (non-oscillatory) behaviour is to abandon the move, remain in the current position, and select a new random direction (Fig. 9b). Diffusion of the collective chemoattractant signal is achieved via a simple 3×3 mean filter kernel with a damping parameter (set to 0.07) to limit the diffusion distance of the chemoattractant.

The low level particle interactions result in complex pattern formation. The population spontaneously forms dynamic transport networks showing complex evolution and quasi-physical emergent properties, including closure of network lacunae, apparent surface tension effects and network minimisation. An exploration of the possible patterning parameterisation was presented in [21]. Although the particle model is able to reproduce many of the network based behaviours seen in the *Physarum* plasmodium such as spontaneous network formation, shuttle streaming and network minimisation, the default behaviour does not exhibit oscillatory phenomena and inertial surging movement, as seen in the organism. This is because the default action when a particle is blocked (i.e. when the chosen site is already occupied) is to randomly select a new orientation—resulting in very fluid network evolution, resembling the relaxation evolution of soap films, and the lipid nanotube networks seen in [27].

The oscillatory phenomena seen in the plasmodium are thought to be linked to the spontaneous assembly / disassembly of actin-myosin and cytoskeletal filament structures within the plasmodium which generate contractile forces on the protoplasm within the plasmodium. The resulting shifts between gel and sol phases prevent (gel phase) and promote (sol phase) cytoplasmic streaming within the plasmodium. To mimic this behaviour in the particle model requires

only a simple change to the motor stage. Instead of randomly selecting a new direction if a move forward is blocked, the particle increments separate internal co-ordinates until the nearest cell directly in front of the particle is free. When a cell becomes free, the particle occupies this new cell and deposits chemoattractant into the lattice (Fig. 9c). The effect of this behaviour is to remove the fluidity of the default movement of the population. The result is a surging, inertial pattern of movement, dependent on population density (the population density specifies the initial amount of free movement within the population). The strength of the inertial effect can be damped by a parameter (pID) which sets the probability of a particle resetting its internal position coordinates, lower values providing stronger inertial movement.

When this simple change in motor behaviour is initiated surging movements are seen and oscillatory domains of chemoattractant flux spontaneously appear within the virtual plasmodium showing characteristic behaviours: temporary blockages of particles (gel phase) collapse into sudden localised movement (solation) and vice versa. The oscillatory domains themselves undergo complex evolution including competition, phase changes and entrainment. We utilise these dynamics below to investigate the possibility of generating useful patterns of regular oscillations which may be coupled to provide motive force.

3.1 Model Setup

The emergence of oscillatory behaviour in the model corresponds to differences in distribution of protoplasm within the plasmodium and subsequent changes in thickness of the plasmodium. In a real *Physarum* plasmodium the changes in thickness of the plasmodium membrane are used to provide impetus (pumping of material through the vein network, or bulk movement of the plasmodium). There is known to be a relationship between the spontaneous contraction of the plasmodium and the subsequent transport of protoplasm away from that region. Thus the region undergoing contraction becomes thinner (allowing more light to pass through when illuminated) and regions away from the contraction become thicker as more protoplasm is present (allowing less light to pass through). In the computational model the transport of particles represents the free flux of protoplasm within the material and the increase in flux (mass particle movement) is indicated in the supplementary video recordings by an increase in greyscale brightness (<http://uncomp.uwe.ac.uk/jeff/engines.htm>). A decrease in the bulk movement of particles represents congestion and a lack of transport and is indicated by a decrease in greyscale brightness (since deposition of chemoattractant factor only occurs in the event of successful forward movement). For clarity in the static images, the greyscale images are inverted (dark areas indicate greater flux).

The particle population's environment is a 2D lattice, represented by a digitised image configured to represent the habitat of the experimental plasmodium. We designed simple shapes in which the particle collective, which composes the virtual material, is confined. The particle population is free to move within unconfined areas. The shapes are composed of 'wall' regions where movement

cannot occur, 'vacant' regions where movement was possible and (where relevant) 'stimulus' regions which provide attraction stimuli, or repulsion stimuli, to the particle population. At the start of each experiment the particle population is randomly distributed through the vacant space in the experimental arena and all particles have random initial orientations. A fixed population size was used (we do not discuss an adaptive population size in this report). The total amount of free possible particle movement is dependent on the population size as a fraction of vacant space. In these results we use a 90% occupancy rate unless otherwise specified, i.e. 90% of all vacant areas are occupied by particles. In all of the experiments there is an initial period where oscillatory behaviour is not initially 'switched on' and this results in self-organised regular domains. When oscillatory motor behaviour is induced these regular domains collapse and the emergence of small domains of regular oscillatory patterns begins. Over time these domains coalesce and compete, causing entrainment of the population into regular oscillation patterns, influenced by both the particle sensory parameters and also by the shape of the experimental arenas.

We use the arena shape to constrain the oscillatory behaviour to ascertain the possibility of utilising the oscillatory behaviours to provide useful 'engine-like' output. By this we mean that the oscillation patterns should be periodic, regular and reliable, in the same way that mechanical engines provide regularly and reliably timed patterns of impetus.

3.2 Data Analysis

We sampled regular frames from the emergent chemoattractant flux patterns and analysed the differences in particle flux by comparing the greyscale levels in different regions of the arena. We were particularly concerned with the reliable initiation of oscillatory behaviour and the characteristics of the behaviour (e.g. the period, the intensity and any coupling effects).

4 Results

We have previously shown that the particle population successfully reproduces the behaviour of the plasmodium when confined within a circular well, resulting in the spontaneous emergence of oscillation patterns (summarised in (Fig. 10)). The type of pattern produced depends on the sensory parameters of each particle (SA and RA parameters) and the SO parameter which, when increased, causes a transition to a different pattern (see [40] for more information). In the circular well the patterns most frequently observed were rotational patterns. When the SO interaction distance was further increased lateral oscillations were observed, followed by an annular pattern. There appears to be a relationship between the circular confining shape of the arena and the type of pattern produced.

We speculate that the reason for the change in pattern type (which, over time, is also observed in the real plasmodium) is that the scale of interactions between the oscillatory regions becomes too large for the circular well, the in-

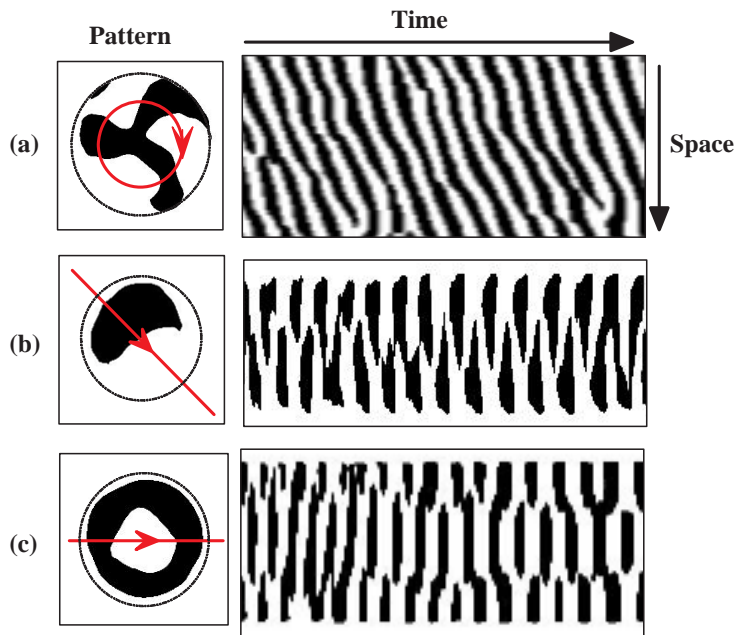


Figure 10: Oscillation patterns observed in a particle model of *Physarum polycephalum* constrained within a circular well. Left: Snapshot of pattern with trajectory of space time plot overlaid, Right: Space time plot of oscillation pattern. a) Rotational pattern, b) Bilateral pattern, c) Annular pattern

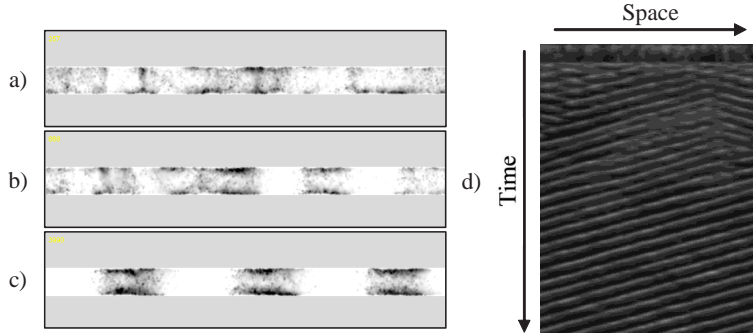


Figure 11: Emergence of travelling wave transport in a tube shaped environment Left: Snapshots taken at a) 257, b) 868 and c) 3990 scheduler steps Right: Space time plot showing emergence of regular transport

teractions are constrained and a new pattern is formed which can 'fit' within the confines of the well. This suggests that the intrinsic oscillations which spontaneously emerge can be shaped in some way by architectural changes to the environment. To further explore this relationship between oscillation pattern type and the environment shape we explored different methods of patterning the virtual arena in order to assess differences in oscillation pattern type and pattern evolution.

4.1 Transport Motion in Open Ended Patterns

We patterned the environment with a simple tube shape whose ends were looped around at the edge of the environment by invoking periodic boundary conditions for the particles. The wall boundaries confined the population to the tube. Snapshots and a space-time plot are shown in Fig. 11. The space time plot is recorded by sampling every pixel along the width of the image at exactly halfway down the tube section and assembling an image based upon these sampled values (pixel brightness is related to chemoattractant trail concentration). After a short period where the non-oscillatory motor condition was used (see top of space-time plot) the oscillatory motor behaviour was initiated. Small domains representing different concentrations of chemoattractant flux appeared (Fig. 11a) which were travelling in different directions. Over time these domains competed and became fewer in number (Fig. 11b) until the tube was evenly divided into regular domains of high flux (regions of free movement) and low flux (regions of obstructed movement). These self-organised domains travelled in a single direction in a regular manner (Fig. 11c and lower section of space-time plot) and are an example of a phase transition into ordered movement patterns as first described in [44].

The travelling waves arising from the collective particle behaviour actually

travel in the opposite direction to the bulk particle motion. In the example shown in Fig. 12 the direction of the travelling wave (Fig. 12b, solid arrow) is right-to-left, whereas the actual movement of the particles (Fig. 12a, dashed arrow) tends to move from left-to-right. Since particles can only move when a space in the lattice becomes available the vacant spaces appear to move in the opposite direction of the particles and the particles themselves show a greater probability of moving when a region of relatively vacant space is near (Fig. 12c, also note that particle movement tends to occur in the lighter regions, which are regions with more vacant space and greater chemoattractant flux). The spaces themselves appear to move backwards because a particle moving from its current position to occupy a vacant space subsequently leaves a new vacant space at its previous position. Because chemoattractant is only deposited by the particles after a successful movement, the chemoattractant flux will be patterned by the distribution of vacant spaces and the wavefront thus moves in the opposite direction to the particles. The bulk movement of the particles is also much slower than the travelling waves, as indicated by Fig. 12, which shows that a single particle takes approximately 8000 scheduler steps to traverse the width of the arena, whereas the travelling wave crosses the arena in approximately 400 steps, a 20:1 difference (although the particle's progress is hindered somewhat by the resistance caused by the low numbers of vacant spaces and changes in direction on contact with the border regions). The opposite direction of the self-organised travelling wave with respect to particle movement is reminiscent of the characteristic backwards propagation seen, for example, in traffic jams [17].

Further analysis of the directional alignment of the particles revealed some unexpected properties of the particle population in relation to the travelling wave. At the start of an experiment the distribution and alignment of the particle population is randomly chosen (Fig. 13a) and the ratio of particles facing left and those facing right is typically equal at 50:50 (we consider particle alignment as being 'left facing' or 'right facing', depending on whether their actual orientation angle falls into either category). When the travelling wave has emerged and stabilised the distribution of the particles is such that they are grouped in regions (Fig. 13b) which are similar - but slightly offset - to the regions of high and low chemoattractant concentration seen in the travelling wave (Fig. 13c). The particles in each region share the same general alignment and the different regions alternate with respect to the alignment of the particles within them (i.e. regions are LEFT, RIGHT, LEFT, RIGHT and so on). The final alignment ratio at the end of an experiment was typically 53:47 (rounded average of ratios over ten runs), with the majority of particles facing in the direction of the travelling wave. The particles change their directional alignment at the same speed as the oncoming travelling wave. The actual movement of the particles, however, is much slower and in the opposite direction to the wave.

Contractile waves travelling along protoplasmic tubes (Fig. 13) can be used to pump liquid substances and, quite likely, to transport fine-grained granular substance. Two examples are shown in Fig. 14, see detailed explanation of experimental setups in [4].

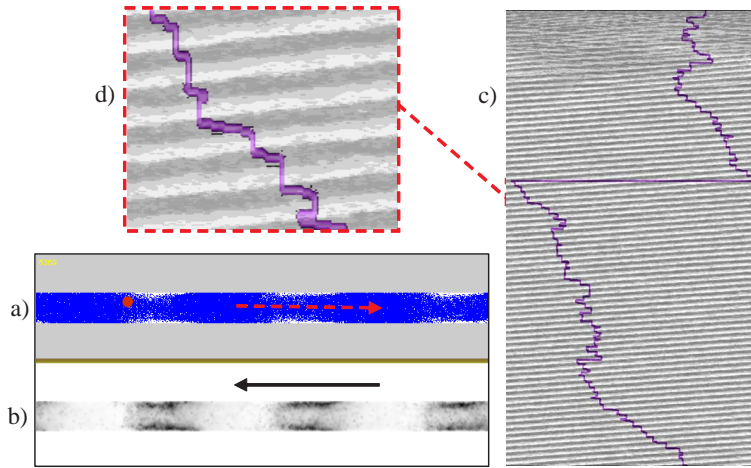


Figure 12: Collective particle drift is opposite to the direction of wave propagation. a) Particle positions and tracer particle (circled), b) Chemoattractant wave propagation, c) Space-time plot overlaid with tracer particle position, d) Enlarged portion showing tracer particle movement (horizontal movement) tends to occur in vacant (high chemoattractant flux) areas.

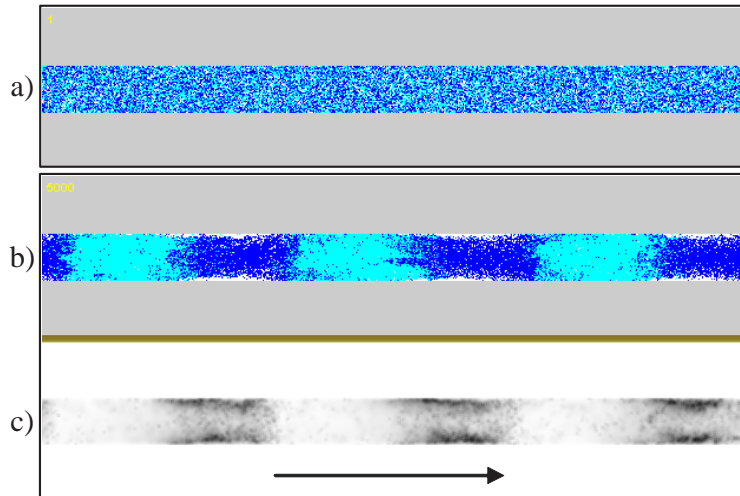
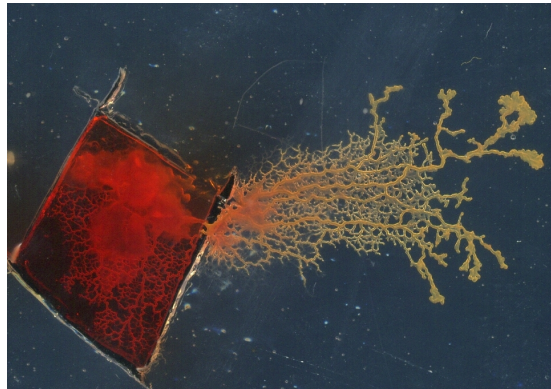
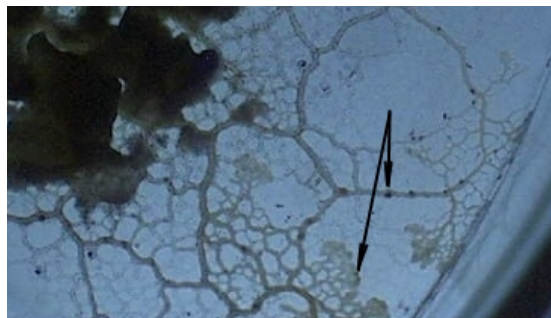


Figure 13: Collective particle alignment and the travelling wave. a) Initial random distribution of particles and their alignments, b) When the stable travelling wave occurs particles are distributed into groups sharing similar directional alignment: lighter regions are oriented to face right and darker regions are oriented leftwards, c) Chemoattractant flux in travelling wave moving to the right.



(a)



(b)

Figure 14: Evidences of *Physarum* transport: (a) Propagating plasmodial localisation transports red dye outside the inoculation site. See details in [3]. (b) Protoplasmic network with clusters of silver spheres transported away from their source. Examples of two clusters are marked by arrows.

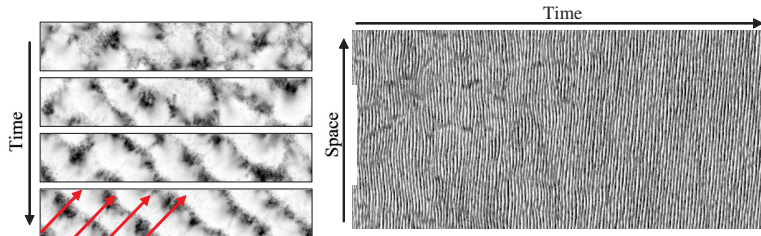


Figure 15: Helical transport in non-patterned environment with periodic boundary conditions. Left: Snapshots of competition and entrainment of wavefronts with final helical-type movement arrowed, Right: Space-time plot showing long period before regular transport occurs.

First example demonstrates pumping of red food colouring along tubes of the growing protoplasmic tree. Initially, a piece of plasmodium was inoculated in the small domain of agar physically insulated from the rest of agar plate. An oat flake saturated with red food colouring is placed nearby the plasmodium, also inside the insulated domain. The plasmodium propagates outside the domain and crosses the agar-less boundary. It pumps the food colouring across the boundary Fig. 14a [3, 4].

Second example deals with transport of granular substances. We mixed an oat flake powder with a small quantity of hollow silver-coated spheres (10-27 μm diameter, Cospheric Inc, Santa Barbara, CA) and inoculated *Physarum* on top of the mixture. Preliminary experiments suggest that the spheres are transported both inside the protoplasmic tubes (usually solitary spheres) and on the outside of the tube's membrane (usually larger conglomerates of spheres) (Fig. 14a).

By patterning the environment to remove all wall boundaries and ensure periodic boundary conditions the emergent oscillatory patterns self-organised into travelling waves (Fig. 15). However there was a much greater length of time needed for the competition between the wave patterns to complete and form synchronous travelling waves. The increase in time before synchronous waves emerge can be explained by the greater initial freedom of movement afforded by the lack of movement constraints from the environment.

By removing the movement at the boundaries and instead patterning the vacant space into looped structures rotary motion of the travelling waves was achieved (Fig. 16). The competition period before synchronisation was relatively brief (Fig. 16a, space-time plot), again because the environmental barriers reduce initial freedom of movement. The looped structures also enabled travelling wave motion even when the environment added non-circular elements, and more tortuous paths (Fig. 16 b and c). The successful initiation of rotary motion suggests the possibility of generating reliable conveyor type transport.

By combining two circular patterns and introducing a region which over-

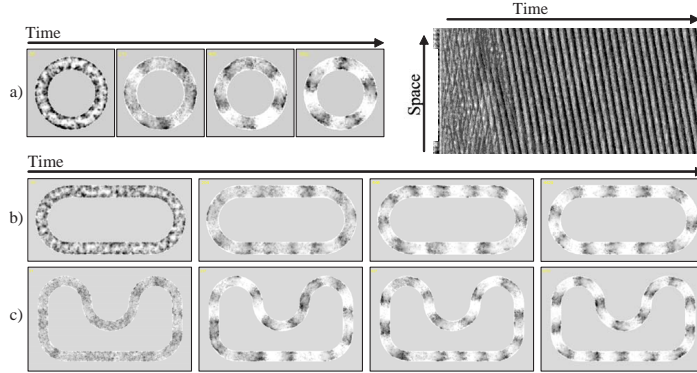


Figure 16: Emergence of rotary motion oscillations. a) Emergence of rotary motion and visualisation of space-time plot showing regular motor pulses. Space time plot was created by recording 360 points inside the vacant track of the circle, b) Tracked rotary movement from a combination of circular and straight regions, c) Conveyor type motion from a more tortuous looped structure.

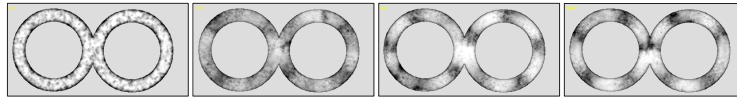


Figure 17: Emergence of gear-like coupling in an overlapping two rotor pattern. Snapshots taken at 20, 121, 981 and 6997 scheduler steps.

lapped and exposed to two separate wavefronts it was possible to achieve entrainment, after 5000 scheduler steps, of the pulses from one rotary 'motor' to another, mimicking the transmission and synchronisation of movement to another ring by a fluidic coupling effect (Fig. 17). Like a conventional gear transmission, the rotation of two facing rings was in opposite directions, however, unlike conventional gear trains, the 'teeth' (wavefront peaks) did not overlap.

To simulate the transport of substances using the emergent travelling waves of the model we computed a vector field based at every scheduler step on instantaneous snapshots of the wave activity (Fig. 18a). The vector field was computed by dividing the habitable areas of the lattice into 15×15 pixel regions. Each vector value was located at the centre of a region and was computed from the difference of chemoattractant flux at extreme borders of each region. The difference between left and right borders giving the \mathbf{dx} value and the differ-

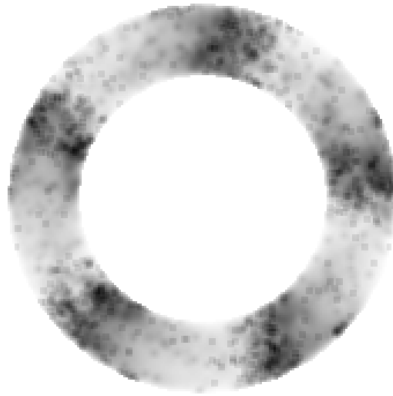
ence between top and bottom borders giving the \mathbf{dy} value. These values were converted to polar coordinates to provide the angle of the strongest local concentration (direction) and the force given to the transported substances. The values within the computed vector field were used to move passive substances, whose locations are represented by the circular areas (Fig. 18b). The supplementary video recording illustrates how information within the travelling wave patterns can be translated into motive force to transport the passive substances. The recording of the vector field also shows the direction and size of the inputs to the transported substances.

4.2 Transport in Closed Path Patterns

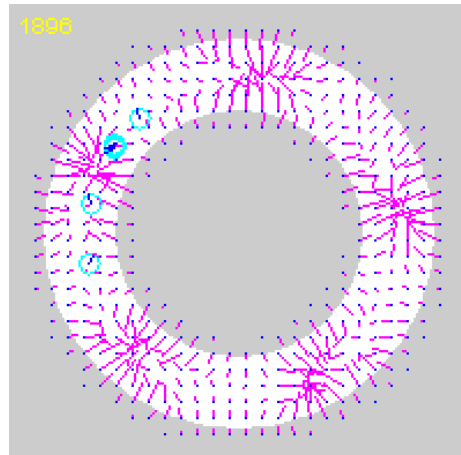
The transport motion in open ended looped patterns stabilises because the bulk particle drift eventually synchronises with the travelling waves. The distribution of the particle population becomes relatively evenly distributed within the path, punctuated by regularly spaced changes of particle occupation density. When closed path patterns were used, however, the uniform distribution cannot occur because separate ends of the path cannot communicate the transport of particles. Thus, over time, the drift of particles results in a tendency for the particle population density to become greater at one end of the chamber. Once there is an imbalance at one end the number of vacant spaces at that end falls and the particles are then attracted to the opposite side of the chamber where more vacant areas exist. Short term oscillatory transport and competition within the chamber still occurs (Fig. 19a and b), as with looped patterns, but this is mediated by a second order of oscillations, which occurs over a much longer timescale since it is caused by the slower bulk drift of particles (Fig. 19c). The effect is regular changes in direction of transport direction and this suggests a possible mechanism of how changes in direction in open-ended looped systems could be achieved - by temporarily introducing a blockage in a looped path until a change in direction occurred.

Another method to confine the collective to a region is by using strong sources of attractant to effectively 'pin down' the collective in place instead of confining it physically within a region by its boundaries. Attractant sources are represented by projecting values at every scheduler step into the chemoattractant diffusion field. These sources diffuse and attract the individual particles of the collective. By spacing the placement of attractants the collective is retained in place in a sheet-like fashion by the attraction of the particles to the sources and the mutual attraction of particles to their own deposition of chemoattractant into the diffusion field (Fig. 20a).

When oscillatory motor behaviour is activated travelling waves of chemoattractant movement emerge in different directions (Fig. 20b). These waves compete for a short time before one direction predominates (Fig. 20c).



(a)



(b)

Figure 18: Simulation of passive transport of substances using information from travelling waves. (a) Spatial representation of snapshot of emergent travelling waves. (b) Computed vector field based upon direction and gradient of travelling waves is used to move passive objects (circular shapes).

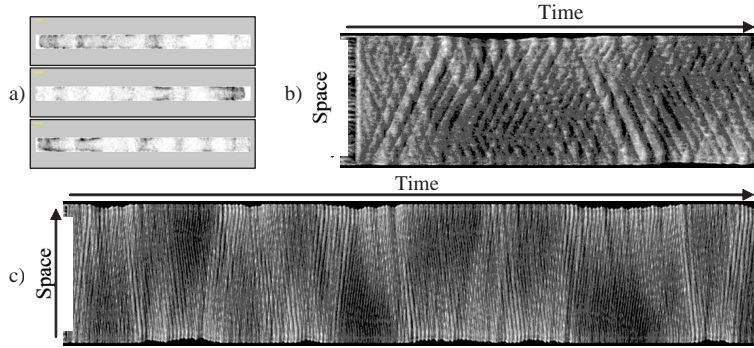


Figure 19: Complex second-order oscillations caused by bulk drift in closed path environments. a) Pulsatile oscillations at different sides of a closed chamber, b) Initial phase of space-time plot showing initiation of oscillatory behaviour and competition between oscillatory domains, c) long term (20,000 steps) space-time plot showing second order oscillations as bulk particle positions oscillate from one side of the chamber to the other. Dark regions at either side of plot indicate periods of second-order oscillations.

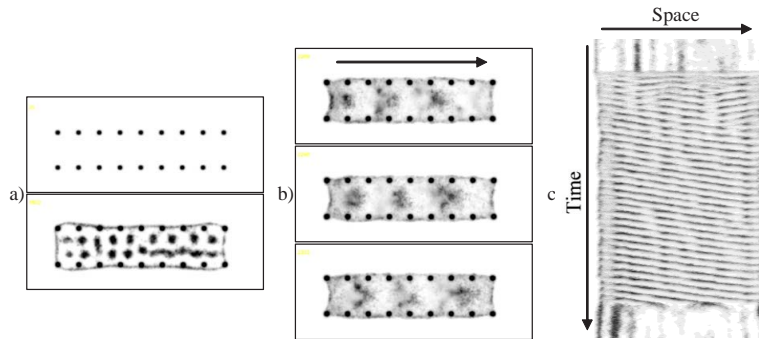


Figure 20: Confining the collective by attractant projection and emergence of travelling wave. a) Regularly spaced projection of chemoattractant sources (top) confines position of collective (bottom), b) When oscillatory motor behaviour is activated a travelling wave emerges across the confined collective, c) Space-time plot of the emergence of travelling waves in a pinned collective.

5 Conclusion and Discussion

We have examined the problem of generating, controlling and distributing motive forces at very small scales using the true slime mould *Physarum polycephalum* as a prototype mechanism. *Physarum* is attractive because it satisfies many physical and computational properties which are desirable in robotics applications (self-oscillatory, simple components, distributed sensory and motor control, integration of multiple sensory stimuli, amorphous and adaptive shape, amenable to external influence, resilience to damage, self repair). Using the organism itself we have demonstrated and measured its ability to lift and pump material using its intrinsic oscillations and protoplasmic streaming. We also investigated mechanisms by which the pumping and transport behaviour may be externally influenced and inhibited, using irradiation stimuli, so that it may be used as a prototype steering mechanism. We used actual experimental data of the bilateral output from a dumbbell shaped plasmodium to drive a model mechanism, a Braitenberg-type vehicle and used the irradiation stimulus to act as a steering force.

In the experiments presented here, the size of *Physarum* cells was about a few millimeter scale. However, the possible minimum size of the *physarum* plasmodium is known to be approximately tens of microns. Considering the size-invariant oscillating behaviour of the *Physarum* slime mould, it should be possible to construct a micron-scale *Physarum* engine to actuate tiny objects.

Moving beyond the use of the plasmodium as a single engine, or pumping, element, we explored how the distributed transport within the organism could be reproduced for synthetic distributed transport. By patterning a densely packed particle population into different shapes we were able to simulate reliable and regular oscillatory movement as emergent travelling waves of plasmodial contractions which were fashioned into rotary, reciprocal, helical, and coupled transport mechanisms. The waves, consisting of peaks and troughs of simulated chemoattractant flux, were found to travel at opposite directions, and with much greater velocity, than the underlying particle drift motion which generated the waves. By computing a simple vector field from the wave motion it was possible to simulate motive forces to transport substances within the environment.

Physarum slime mould is an organism which efficiently exploits self-oscillatory phenomena to transport nutrients within its protoplasmic network and can inspire material approaches to distributed movement and transport. We envisage that these prototype results of our studies on slime-mould engines and transporting devices could be applied in the design and manufacturing of intelligent soft manipulator arrays in micro-electronic assembly, drug delivery systems and novel prototypes of artificial tissue and organs.

6 Acknowledgement

The work was partially supported by the Leverhulme Trust research grant F/00577/1 “Mould intelligence: biological amorphous robots”. Experiments

in Section 2.2 was conducted in Prof Hywel Morgan’s lab at University of Southampton as a part of the project supported by the Life Sciences Interfaces Forum (Project manager: Dr Klaus-Peter Zauner).

References

- [1] Adamatzky A. Physarum machines: encapsulating reaction-diffusion to compute spanning tree. *Naturwissenschaften*, 94(12):975–980, 2007.
- [2] Adamatzky A. Physarum boats: if plasmodium sailed it would never leave a port. *Applied Bionics and Biomechanics*, 7(1):31–39, 2010.
- [3] A. Adamatzky. Manipulating substances with physarum polycephalum. *Materials Science & Engineering C*, 38(8):1211–1220, 2010.
- [4] A. Adamatzky. *Physarum Machines*. World Scientific, 2010.
- [5] A Adamatzky, P Arena, A Basile, R Carmona-Galan, BDL Costello, L Fortuna, M Frasca, and A Rodriguez-Vazquez. Reaction-diffusion navigation robot control: from chemical to vlsi analogic processors. *Circuits and Systems I: Regular Papers, IEEE Transactions on [see also Circuits and Systems I: Fundamental Theory and Applications, IEEE Transactions on]*, 51(5):926–938, 2004.
- [6] A. Adamatzky, B. de Lacy Costello, S. Skachek, and C. Melhuish. Manipulating objects with chemical waves: Open loop case of experimental belousov-zhabotinsky medium coupled with simulated actuator array. *Physics Letters A*, 350(3-4):201–209, 2006.
- [7] A Adamatzky, Ben De Lacy Costello, and T Shirakawa. Universal computation with limited resources: Belousov-zhabotinsky and physarum computers. *International Journal of Bifurcation and Chaos*, In Press, 2008.
- [8] A. Adamatzky and J. Jones. Towards Physarum robots: computing and manipulating on water surface. *Journal of Bionic Engineering*, 5(4):348–357, 2008.
- [9] B.Q. Ai, H.Z. Xie, D.H. Wen, X.M. Liu, and L.G. Liu. Heat flow and efficiency in a microscopic engine. *The European Physical Journal B*, 48(1):101–106, 2005.
- [10] P.J. Allen and W.H. Price. The relation between respiration and protoplasmic flow in the slime mold, Physarum polycephalum. *American Journal of Botany*, 37(5):393–402, 1950.
- [11] J. D Anderson. Galvanotaxis of slime mold. *J. Gen. Physiol.*, 35(5):1–1, 1951.

- [12] V. Braitenberg. *Vehicles: Experiments in Synthetic Psychology*. MIT Press, Cambridge, MA, 1984.
- [13] J. den Toonder, F. Bos, D. Broer, L. Filippini, M. Gillies, J. de Goede, T. Mol, M. Reijme, W. Talen, H. Wilderbeek, et al. Artificial cilia for active micro-fluidic mixing. *Lab Chip*, 8(4):533–541, 2008.
- [14] R.H. Dillon, L.J. Fauci, C. Omoto, and X. Yang. Fluid dynamic models of flagellar and ciliary beating. *Annals of the New York Academy of Sciences*, 1101(Reproductive Biomechanics):494–505, 2007.
- [15] R. Dreyfus, J. Baudry, M.L. Roper, M. Fermigier, H.A. Stone, and J. Bibeute. Microscopic artificial swimmers. *Nature*, 437(7060):862–865, 2005.
- [16] R.S. Fearing. Survey of sticking effects for micro parts handling. In *Intelligent Robots and Systems 95. Human Robot Interaction and Cooperative Robots*, *Proceedings. 1995 IEEE/RSJ International Conference on*, volume 2, pages 212–217. IEEE, 2002.
- [17] M. R. Flynn, A. R. Kasimov, J. C. Nave, R. R. Rosales, and B. Seibold. Self-sustained nonlinear waves in traffic flow. *Physical Review E*, 79(5):56113, 2009.
- [18] K. Gotoh and K. Kuroda. Motive force of cytoplasmic streaming during plasmodial mitosis of physarum polycephalum. *Cell Motility and the Cytoskeleton*, 2(2):173–181, 1982.
- [19] D.-P. Häder and T Schreckenbach. Phototactic Orientation in Plasmodia of the Acellular Slime Mold , Physarum polycephalum. *Cell*, 25(1):55–61, 1984.
- [20] A.J. Ijspeert. Central pattern generators for locomotion control in animals and robots: a review. *Neural Networks*, 21(4):642–653, 2008.
- [21] J. Jones. Characteristics of pattern formation and evolution in approximations of physarum transport networks. *Artificial Life*, 16(2):127–153, 2010.
- [22] J. Jones. The emergence and dynamical evolution of complex transport networks from simple low-level behaviours. *International Journal of Unconventional Computing*, 6(2):125–144, 2010.
- [23] N. Kamiya. The protoplasmic flow in the myxomycete plasmodium as revealed by a volumetric analysis. *Protoplasma*, 39(3):344–357, September 1950.
- [24] N. Kamiya and K. Kuroda. Studies on the velocity distribution of the protoplasmic streaming in the myxomycete plasmodium. *Protoplasma*, 49(1):1–4, March 1958.

- [25] C.R. Kubea and E. Bonabeaub. Cooperative transport by ants and robots. *Robotics and autonomous systems*, 30:85–101, 2000.
- [26] Istvan Lagzi, Siowling Soh, Paul J. Wesson, Kevin P. Browne, and Bartosz A. Grzybowski. Maze solving by chemotactic droplets. *Journal of the American Chemical Society*, 2010. doi: 10.1021/ja9076793.
- [27] T. Lobovkina, PG Dommersnes, S. Tiourine, J.F. Joanny, and O. Orwar. Shape optimization in lipid nanotube networks. *The European Physical Journal E: Soft Matter and Biological Physics*, 26(3):295–300, 2008.
- [28] Tatsiana Lobovkina, Irep Gozen, Yavuz Erkan, Jessica Olofsson, Stephen G. Weber, and Owe Orwar. Protrusive growth and periodic contractile motion in surface-adhered vesicles induced by ca^{2+} -gradients. *Soft Matter*, 6(2):268–272, 2010.
- [29] S. Maeda, Y. Hara, T. Sakai, R. Yoshida, and S. Hashimoto. Self-Walking Gel. *Advanced Materials*, 19(21):3480–3484, 2007.
- [30] T. Nakagaki, S. Uemura, Y. Kakiuchi, and T. Ueda. Action spectrum for sporulation and photoavoidance in the plasmodium of *Physarum polycephalum*, as modified differentially by temperature and starvation. *Photochem. Photobiol.*, 64(5):859–862, 1996.
- [31] T. Nakagaki, H. Yamada, and T. Ueda. Modulation of cellular rhythm and photoavoidance by oscillatory irradiation in the *Physarum* plasmodium. *Biophysical Chemistry*, 82:23–28, 1999.
- [32] N. Saga and T. Nakamura. Development of a peristaltic crawling robot using magnetic fluid on the basis of the locomotion mechanism of the earthworm. *Smart Materials and Structures*, 13:566, 2004.
- [33] I. Sher, D. Levinzon-Sher, and E. Sher. Miniaturization limitations of HCCI internal combustion engines. *Applied Thermal Engineering*, 29(2-3):400–411, 2009.
- [34] D.A. Smith and R Saldana. Model of the Ca^{2+} oscillator for shuttle streaming in *Physarum polycephalum*. *Biophysical journal*, 61(2):368–80, February 1992.
- [35] JW Suh, RB Darling, K.F. Bohringer, BR Donald, H. Baltes, and GT Kovacs. Fully programmable MEMS ciliary actuator arrays for micromanipulation tasks. In *Robotics and Automation, 2000. Proceedings. ICRA'00. IEEE International Conference on*, volume 2, pages 1101–1108. IEEE, 2002.
- [36] S. Takagi and T. Ueda. Emergence and transitions of dynamic patterns of thickness oscillation of the plasmodium of the true slime mold *Physarum polycephalum*. *Physica D*, 237:420–427, 2008.

- [37] A. Takamatsu and T. Fujii. Construction of a living coupled oscillator system of plasmodial slime mold by a microfabricated structure. *Sensors Update*, 10(1):33–46, January 2002.
- [38] A. Takamatsu, T. Fujii, and I. Endo. Control of interaction strength in a network of the true slime mold by a microfabricated structure. *BioSystems*, 55:33–38, 2000.
- [39] B.A. Trimmer, A.E. Takesian, B.M. Sweet, C.B. Rogers, D.C. Hake, and D.J. Rogers. Caterpillar locomotion: A new model for soft-bodied climbing and burrowing robots. In *7th International Symposium on Technology and the Mine Problem*. Citeseer, 2006.
- [40] S. Tsuda and J. Jones. The emergence of complex oscillatory behaviour in *physarum polycephalum* and its particle approximation. In *Artificial Life XII*, pages 698–705, 2010.
- [41] S. Tsuda and J. Jones. The emergence of synchronization in *physarum polycephalum* and its particle approximation. *Biosystems*, 2010. (submitted).
- [42] S. Tsuda, K.-P. Zauner, and Y.-P. Gunji. Robot control with biological cells. In *Proceedings of the Sixth Int. Workshop on Information Processing in Cells and Tissues, Aug. 30–Sept. 1, 2005, St. William’s College, York*, pages 202–216, 2005.
- [43] T. Umedachi, T. Kitamura, K. Takeda, T. Nakagaki, R. Kobayashi, and A. Ishiguro. A Modular Robot Driven by Protoplasmic Streaming. *Distributed Autonomous Robotic Systems 8*, pages 193–202, 2009.
- [44] T. Vicsek, A. Czirók, E. Ben-Jacob, I. Cohen, and O. Shochet. Novel type of phase transition in a system of self-driven particles. *Physical Review Letters*, 75(6):1226–1229, 1995.
- [45] K. E. Wohlfarth-Bottermann. Oscillating contractions in protoplasmic strands of *physarum*: simultaneous tensiometry of longitudinal and radial rhythms, periodicity analysis and temperature dependence. *Journal of Experimental Biology*, 67:49–59, 1977.
- [46] R. Wolf, J. Niemuth, and H. Sauer. Thermotaxis and protoplasmic oscillations in *Physarum* plasmodia analysed in a novel device generating stable linear temperature gradients. *Protoplasma*, 197(1-2):121–131, March 1997.
- [47] Y. Yoshimoto and N. Kamiya. Studies on contraction rhythm of the plasmodial strand iii. role of endoplasmic streaming in synchronization of local rhythms. *Protoplasma*, 95:111–121, 1978.
- [48] L. Zhang, J.J. Abbott, L. Dong, B.E. Kratochvil, D. Bell, and B.J. Nelson. Artificial bacterial flagella: Fabrication and magnetic control. *Applied Physics Letters*, 94(6):064107, 2009.

- [49] S. Zhang. Fabrication of novel biomaterials through molecular self-assembly. *Nature biotechnology*, 21(10):1171–1178, 2003.